Optimal pass planning for robotic welding of large-dimension joints with nonuniform grooves

SJ Yan, HC Fang, SK Ong and AYC Nee

Abstract

Large-dimension welded joints are widely used in shipyards and oilfields. These joints typically have thick and nonuniform welding grooves, thus requiring multi-pass welding processes and tens of hours to complete. Although the development of robotic welding systems can shorten the welding time, it is important to have a detailed plan of the entire process before welding starts. Welding pass planning is crucial for the subsequent robot trajectory generation and provides the welding sequence in a deep groove and the welding parameters of every pass. A knowledge database is used in this research to obtain the relationship between the bead geometry and the welding parameters. A layer-by-layer welding pass planning scheme is proposed to address the nonuniform groove geometry, and an optimization method is proposed with the objective to maximize the section area of the weld bead, so that the number of passes can be minimized. The planning results show that the optimization method is able to provide feasible passes and welding parameters for every pass.

Introduction

In shipyards and oilfields, it is common to have large-dimension welded joints consisting of thick plates or pipes. Single-pass welding cannot fill the deep grooves of these joints. Correspondingly, multi-pass welding becomes necessary, and manual methods are usually used. The process of manual methods includes preheating, flame cutting, grinding, arc welding, post-heating, polishing and so on. In order to achieve good quality, the entire process poses high requirements on the welding technicians, and it is difficult to achieve high productivity. With the advancement of robotic welding processes, high accuracy and high efficiency have become possible for the welding of deep grooves.

For robotic welding systems, welding task planning is important to welding quality and efficiency. Hence, it has drawn many researchers' attention.[1–4] Offline robot programming methods are still the most prevalent for robot welding task planning and simulation prior to converting the welding passes into robot welding paths. Augmented reality (AR)–based robot programming methods[5–7] improve offline programming by allowing adequate human intervention through which the task can be planned, modified, simulated and visualized in an augmented environment.

Welding of deep grooves requires multiple passes to fill up the groove section. To realize automatic welding solutions, precise pass planning is critical to provide welding sequence and route and subsequently robotic trajectory. Park and An[8] reported that a welding sequence can have a significant effect on welding distortion, which would subsequently affect the welding quality. Recent studies have been reported on the development of welding knowledge databases through capturing human welders' behavior to facilitate welding process automation.[9,10] In these approaches, manual welding expertise can be modeled to assist the selection of welding parameters and settings in robotic welding.

Department of Mechanical Engineering, Faculty of Engineering, National University of Singapore, Singapore

Corresponding author:
SK Ong, Department of Mechanical Engineering, Faculty of Engineering, National University of Singapore, 9 Engineering Drive 1, 117576 Singapore.
Email: mpeongsk@nus.edu.sg

A number of research works have been studied on different weld bead modeling approaches in welding pass planning. Yang et al.[2] introduced a planning method by simplifying weld beads to be parallelograms or trapezoids, and these parallelograms or trapezoids are placed into a deep groove until the groove is filled. This method simplifies the geometry of the weld bead; however, it is not accurate to use parallelograms or trapezoids as the section shape of a single weld bead is obviously different from a parallelogram or trapezoid. In order to approximate the bead section using regular curves, Cao et al.[11] investigated Gaussian, logistic, parabola and sine functions. Experimental results show that the sine function has the highest fitting accuracy to the bead section. Nevertheless, the parabola function was found to be more accurate than a cosine function, which has the same shape as a sine function, according to the experimental results done by Xiong et al.[12] The parabola function was also adopted by Suryakumar et al.,[13] and experimental results showed low errors. Although accurate approximations of bead sections have been used,[11–13] their works focused on pass planning on flat plates without limitations posed by the groove edges.

The approximation of bead sections is an important step in pass planning, but it should be noted that the bead shapes are dependent on welding parameters and properties of the base and filler metals. This dependence has been studied by many researchers. Yang et al.[2] and Suryakumar et al.[13] used induced equations to relate bead sections with welding parameters. These induced equations can obtain the approximate section areas using wire feed rate, wire diameter and welding speed; however, it is known that the bead shape is also related to the current, voltage, shielding gas and other welding parameters. Therefore, it is difficult to achieve good accuracy using induced equations. As compared with the approximate equations, experimental methods have been reported to achieve better accuracy. Regression analysis[14–22] and artificial neural networks (ANNs)[17,20,22–27] have been used widely to model the

relationship between bead geometry and welding parameters based on experimental data. According to Xiong et al.,[17] Kim et al.[20] and Lee and Um,[22] ANNs show superior performance to regression analysis in predicting accuracy. Although good accuracy can be achieved using experimental methods, their performance is highly dependent on experimental data. The corresponding models can guarantee the accuracy only in similar welding environments, such as the same base metal and filler metal, the same welding method, similar ventilation.

In this research, a welding knowledge database is created to model the relationship between bead geometry and various welding parameters. This model is used to select feasible welding parameters during pass planning for nonuniform grooves. A layer-by-layer pass planning scheme is proposed on the basis that the number of pass layers for a given groove segment does not have to be equal. This scheme addresses the possible needs for significant changes in weld bead dimensions within a layer across all the cross sections in the segment by increasing the number of layers in the deeper groove region. A weighted average optimization method is proposed to determine the minimum number of passes to fill the given segment and ensure that every weld bead can be achieved using the selected welding parameters.

Knowledge database for welding

The knowledge database in this research contains experimental data collected from automatic welding processes. Manual welding method is not considered since several welding parameters, such as the welding speed which is crucial to the welding quality, cannot be controlled precisely during the manual welding process. The database consists of five different components, which are the welding method, base metal, filler metal, welding parameters and responses. The welding method can be metal inert gas welding or metal active gas welding. The properties of the filler metals include the information of the metal grade, materials and dimensions. Figure 1 shows the elements and their properties
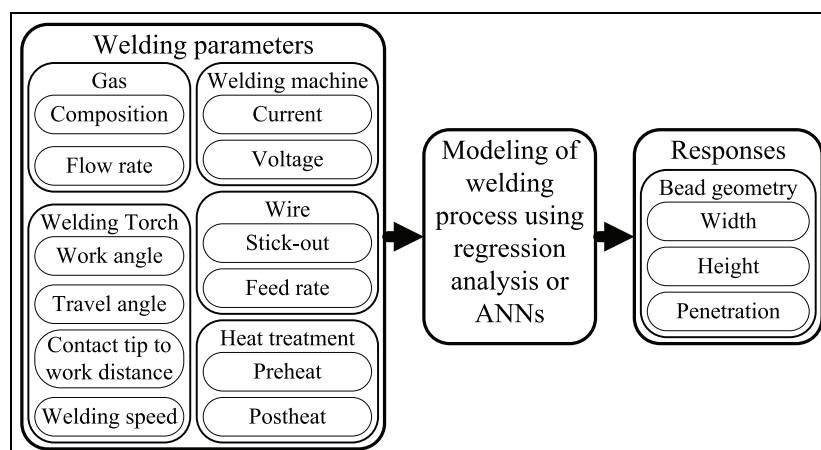

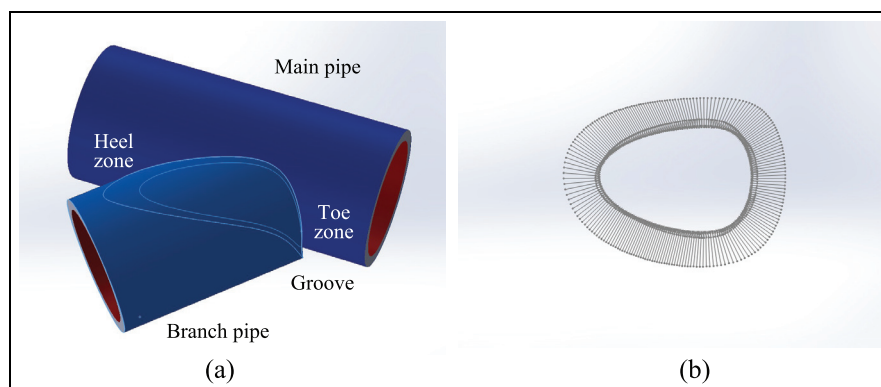**Figure 1.** The inputs and outputs of the modeling of welding process.

Figure 2. Scaled-down Y-joint structure: (a) CAD model and (b) welding groove with bisector direction.

contained in the welding parameters component and the responses component. The responses component has one element which is the bead geometry characterized by the bead width, bead height and bead penetration.

With the database, the relationship between the welding parameters and the geometry can be modeled using regression analysis or ANNs. For many combinations of the base and filler metals, it is common to have several parameters that do not change and remain constant. Hence, the parameters are categorized into constants and variables during the modeling process. The modeling results show implicit or explicit functions of the variable parameters, while constant parameters provide reference to the conditions. The relationship can also be built using a selective combination of variable parameters for different welding settings in which all the welding parameters may not be independent of each other, for instance, arc voltage and feed rate are set to be dependent on welding current in many welding equipments. In this research, however, three welding parameters, namely, welding speed, welding current and arc voltage, are used to establish the weld bead model, and they can be defined independently.

Pass planning for nonuniform groove geometry

Welding groove representation and groove segmentation

Figure 2(a) depicts a computer-aided design (CAD) model of a scaled-down Y-joint structure, which consists of a *main* pipe and a *branch* pipe with a 45° intersection angle between the two pipes. Figure 2(b) defines the corresponding welding groove model using a sequence of cross sections, with the bisector direction at each cross section separating the groove angle (or joint-included angle) into two equal bevel angles. For a uniform groove, as investigated in Yang et al.[2] and Yan et al.,[28] welding pass planning can be reduced to pass layout planning for one cross section. In this research, pass planning to fill up a nonuniform groove is
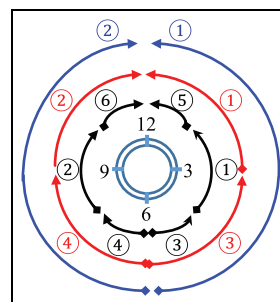

Figure 3. Groove segmentation scheme with uphill welding direction.

formulated to pass layout planning for a group of cross sections.

The groove geometry of a Y-joint is nonuniform due to the presence of the varied groove angles and groove depths along the groove. Therefore, it is necessary to have multiple welding segments in order to have a more consistent welding pass solution. This is also in accordance with manual welding practices to reduce possible distortion in the welding zone.[29] Criteria for identifying welding segments are the reachability of a welding robot being used, welding position, groove angle or groove width variations. The groove angles are wider at the toe zone, while the groove depths are deeper at the heel zone. If an uphill welding direction is allowed only, at least two segments are needed. Typical numbers of segments are 2, 4 or 6, as illustrated in Figure 3. Having too many segments is not recommended as this would introduce extra welding breaks, leading to a higher possibility of porosity which can compromise the welding quality.

Welding bead model

Before pass planning, three assumptions have been made in this research. They are (1) the weld bead section can be approximated using a parabola function; (2) the overlapped area between adjacent passes or between the weld pass and the groove edge can be added into the valley area; and (3) the bead shape remains the same when
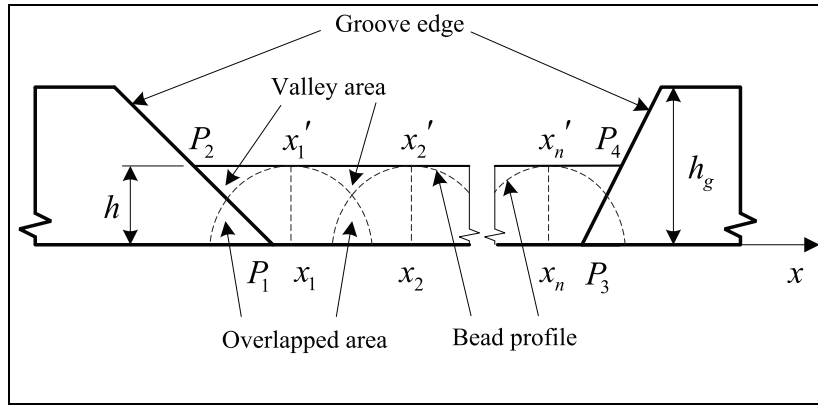
Figure 4. The pass planning of a single layer in a groove cross section.

welding parameters are not changed. According to Xiong et al.,[12] a parabola function can be used to approximate the weld bead section accurately. Therefore, the bead shape is represented using equation (1) where h and w denote the bead height and width, respectively

$$y = -\frac{4h}{w^2}x^2 + h \qquad (1)$$

Figure 4 depicts the overlapped area and valley area in the second assumption. The experiments reported by Cao et al.[11] and Xiong et al.[12] show small deviation from the predicted results using the second assumption. In order to maintain a flat surface for each layer, the bead heights of all the passes in a layer should be the same and the overlapped area should be equal to the valley area. Figure 4 shows the section view of a single layer of a groove which is to be filled. If n denotes the number of passes in the layer; w_i denotes the bead width of the ith pass; x_i specifies the location of the ith pass in the x direction; S denotes the area; and P_1, P_2, P_3 and P_4 denote the intersection points of the layer surfaces and the groove edges, equation (2) can be obtained from equal overlapped area and valley area

$$\begin{cases} S_{P_1 x_1 x_1' P_2} = \dfrac{w_1 h}{3} \\ S_{x_1 x_2 x_2' x_1'} = \dfrac{w_1 + w_2}{3} h \\ S_{x_{n-1} x_n x_n' x_{n-1}'} = \dfrac{w_{n-1} + w_n}{3} h \\ \qquad \vdots \\ S_{x_n P_3 P_4 x_n'} = \dfrac{w_n h}{3} \end{cases} \qquad (2)$$

In equation (2), the unknown variables include w_i and x_i if the number n and bead height h have been defined. The number of unknown variables is $2n$, but equation (2) has $n + 1$ linear equations. If $n > 1$, various solutions can be obtained. In order to guarantee a unique solution, the bead widths of all the passes in a layer are required to be equal. If the groove edges are

straight lines and x_{Pi} denotes the x coordinate of the intersection point P_i, equation (3) can be obtained

$$\begin{cases} w = \dfrac{3(x_{P3} + x_{P4} - x_{P1} - x_{P2})}{4n} \\ x_1 = \dfrac{(2n - 1)(x_{P1} + x_{P2}) + (x_{P3} + x_{P4})}{4n} \\ x_i = x_1 + \dfrac{2}{3} w \end{cases} \qquad (3)$$

Welding pass planning scheme for a groove segment

Each groove segment can be represented by a cluster of cross sections with an uphill sequence. For a uniform welding groove, the pass planning process can be reduced to pass layout planning to fill the weld bead in a cross section, and the number of layers and the number of welding passes can be maintained in the rest of the cross sections without changes in the welding parameters. However, this scheme will fail to plan the passes for a nonuniform groove as it will either end up with too many segments or require significant adjustment of the welding parameters in order to generate the varied size of the welding bead along the pass. As shown in Figure 5(a), the height of the welding beads from the start to the end of the given segment would need to be reduced significantly to achieve equal number of layers; this will, in turn, demand the associated welding parameters to be changed to weld this particular pass. Modern robotic welding systems can alter welding parameters during a single welding pass, but this is not recommended as this could affect welding penetration, etc. which may result in a low quality weldment.

With these considerations, a layer-by-layer pass planning scheme is proposed, as illustrated in Figure 5(b), in which the number of pass layers for all the cross sections along a given segment does not have to be equal. During the planning of the current layer, the number of passes is maintained, and suitable bead heights and bead widths are searched to fill the groove without considering the requirement for the following
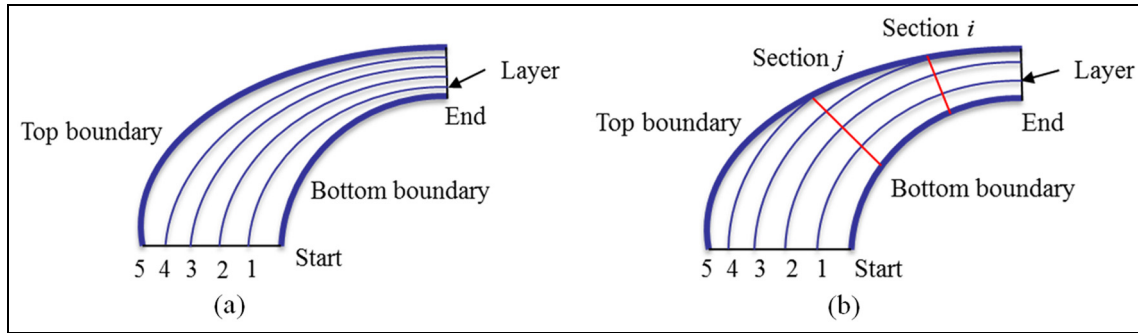
Figure 5. Pass planning schemes in welding a segment: (a) maintain equal number of layers and passes and (b) maintain equal number of passes in each layer.

layers. Weaving technique is allowed to accommodate variable groove widths during welding planning. After the current layer, the sections which have been filled up will be excluded in the planning of the next layer. Due to the uncertainty of the following layers, the final layer may exceed the top boundary of the groove. In this research, it is assumed to be allowed since in practice, cap passes will be needed as the final layer on top of the filling passes to complete the welding.

Optimization of pass planning

Pass planning for a groove segment involves two levels of optimization, namely, local optimization with respect to individual cross section and global optimization with respect to the groove segment. Figure 6 presents a flowchart for pass planning and optimization for a groove segment.

Pass optimization in individual cross section

The objective of pass planning optimization for a single cross section is to fill the section using the minimal number of passes since fewer numbers can increase welding efficiency and decrease the possibility of producing defects among adjacent passes. In order to achieve this goal, the section area of the weld bead can be maximized, as a larger weld bead can decrease the number of passes in a defined groove. Hence, the objective function is to maximize equation (4), where x_{Pi} is dependent on the groove shape and the bead height. The variables include h and n

$$S = \frac{h}{n}(x_{P3} + x_{P4} - x_{P1} - x_{P2}) \qquad (4)$$

During maximization, n must be a positive integer and the values of h and w are subject to the constraint that the bead shape can be achieved using feasible welding parameters. With the knowledge database introduced in section "Knowledge database for welding," the relationship between the bead height h, bead width w and welding parameter vector $\mathbf{V}$ can be modeled using $H(\mathbf{V})$ and $W(\mathbf{V})$. If $\mathbf{B}$ denotes the range of the welding parameters, the constraint can be formulated to be the following expression

$$\exists \mathbf{V} \in \mathbf{B} : [H(\mathbf{V}) - h]^2 + [W(\mathbf{V}) - w]^2 = 0 \qquad (5)$$

Since the bead width w can be obtained using equation (3), the optimization can be specified using equation (6), if ε denotes the tolerance defined by the users, and h_g denotes the distance between the bottom surface of the current layer and the top surface of the groove (Figure 4)

$$\max \frac{h}{n}(x_{P3} + x_{P4} - x_{P1} - x_{P2}) \text{ such that}$$

$$\begin{cases} n \in \mathbf{Z}^+ \\ h - h_g < \varepsilon \\ \exists \mathbf{V} \in \mathbf{B} : [H(\mathbf{V}) - h]^2 \\ \quad + \left[W(\mathbf{V}) - \frac{3(x_{P3} + x_{P4} - x_{P1} - x_{P2})}{4n} \right]^2 < \varepsilon \end{cases}$$

$$(6)$$

Pass optimization for a groove segment

The goal of pass optimization for a groove segment is the determination of the minimum number of passes to fill up the segment subject to the conditions that each pass can be generated with a set of consistent welding parameters. The overall optimization problem consists of optimization of four objectives, namely, (1) minimization of the difference between the desired values and predicted values of bead height, (2) minimization of the difference between the desired values and predicted values of bead width, (3) minimization of the variations of welding speed and weave width in one pass and (4) maximization of the total areas of bead sections for each welding pass. The third objective tends to select similar bead height and width to reduce the variation in welding speed and weave width; however, considering the variations in groove depth at different groove cross sections, the bead height is expected to be larger at the deeper location while the bead width is expected to be smaller at the narrower location. Besides this constraint, other constraints are the upper and lower boundaries defined in the variables, including bead height and welding parameters. The number of passes in the current planning layer should be an integer. Equation (7)
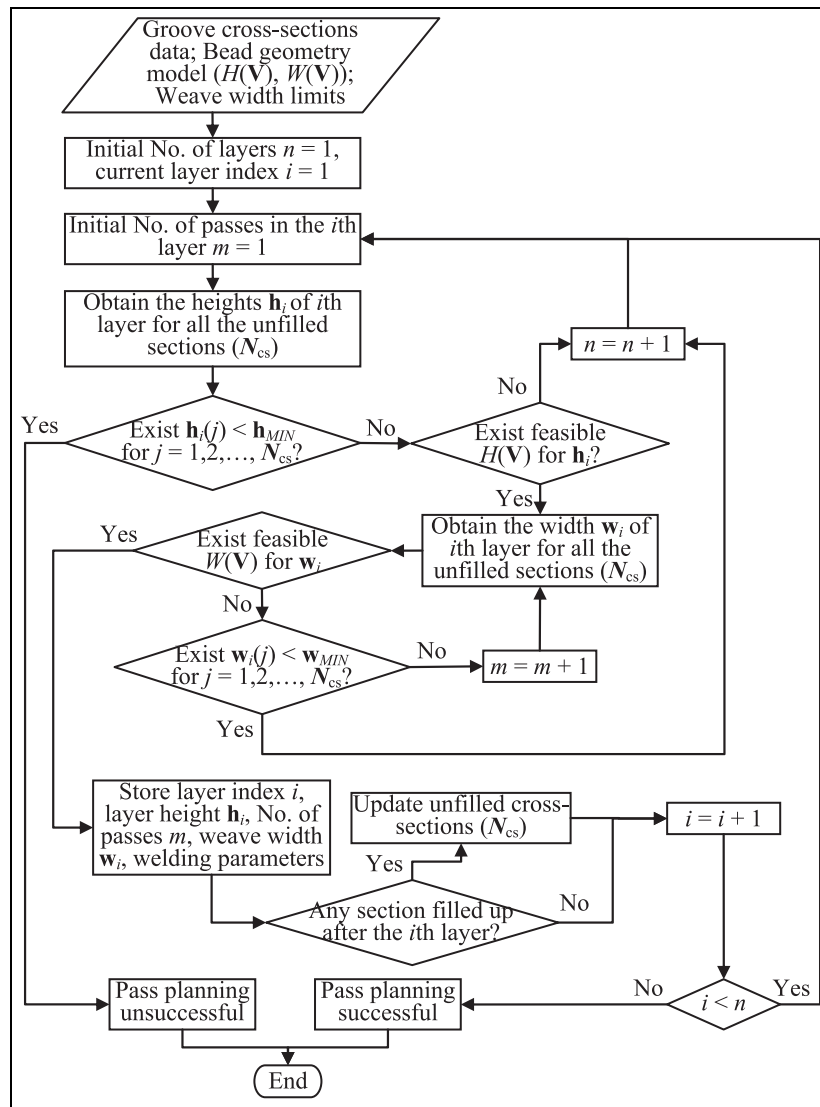
Figure 6. The flowchart of optimal pass planning for a groove segment.

is the final objective function, where f_h is referred to the square root of the square sum of the differences of bead height, f_w is the square root of the square sum of the differences of bead width, f_p is the sum of standard deviations of welding speed and weave width and f_a is the reciprocal of the mean of the areas of bead sections

$$f = \omega_h f_h + \omega_w f_w + \omega_p f_p + \omega_a f_a \qquad (7)$$

In equation (7), ω_h, ω_w, ω_p and ω_a are the weighted coefficients for the four objectives, respectively. The selection of these coefficients is based on the relative importance of these objectives. For instance, the difference between the desired value and the predicted value of bead height can be made up by the following layer; the difference is not as important as that of the bead width. The maximization of bead sections aims to decrease the number of layers. Therefore, these two objectives are comparatively less important. The minimization of the variations of speed and weave width

aims to smoothen these two parameters, which is important for a consistent and smooth bead shape generated along the pass.

Case study and discussion

Pass planning of top-half groove

The CAD model of a Y-joint structure case study is shown in Figure 2(a). The two pipes have the same dimension, each with an inner diameter of 230 mm and an outer diameter of 327 mm, and the intersecting angle between the two pipes is 45°. As the axes of the two pipes are intersecting, the geometry of the top-half and the bottom-half of the groove model is symmetrical. Therefore, only the passes for the top-half of the groove are planned and optimized by addressing the variations in the groove angle and the groove depth. The top-half of the groove is modeled with 51 evenly distributed cross sections, which are further grouped into two segments, namely, toe segment and heel segment, as described in Figure 7.
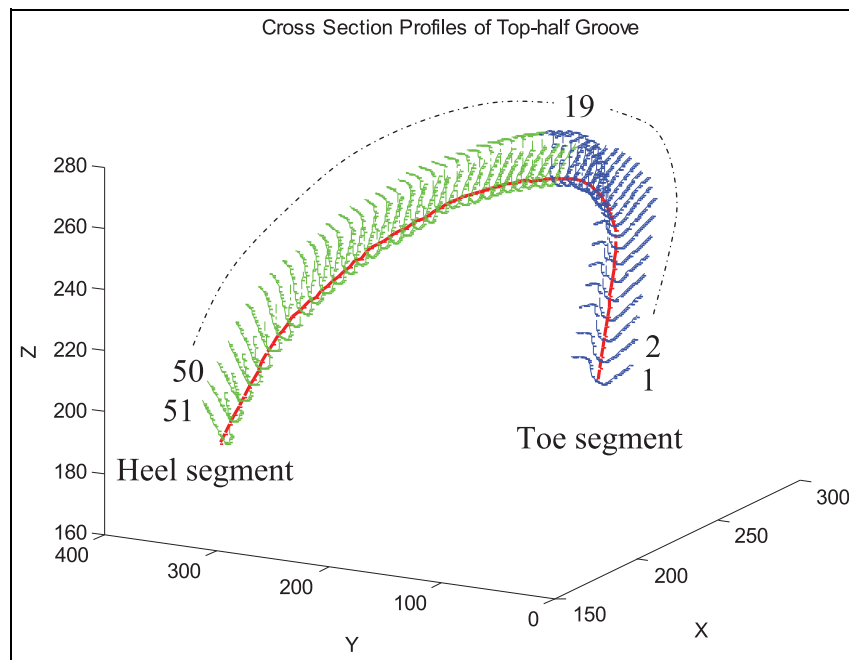
Figure 7. Groove representation with cross sections (top-half groove).

A group of experimental data in the database is used to develop the prediction model of the weld bead geometry. The experiment uses a mild steel plate as the base metal. The filler metal is steel wire with diameter of 1.2 mm. Pure argon is employed as the shielding gas. Table 1 lists the values of the welding current, voltage and speed and the corresponding bead heights and widths. With the experimental data, equation (8) is obtained using regression analysis where I denotes the current, V denotes the voltage and v denotes the welding speed

$$\begin{cases} h = 2.6964 - 0.0031v - 0.0571V + 0.0077I \\ \quad + 6.6 \times 10^{-5}vV - 1.6 \times 10^{-4}VI \\ w = 0.8523 + 2.0 \times 10^{-4}v + 0.1338V + 0.0045I \\ \quad -1.7 \times 10^{-4}vV - 8.0 \times 10^{-6}vI + 1.6 \times 10^{-4}VI \end{cases}$$

(8)

From Table 1, it can be seen that the ranges of speed, voltage and current are $250 \leqslant v \leqslant 410$, $20 \leqslant V \leqslant 30$ and $180 \leqslant I \leqslant 360$. Figure 8 shows the comparison between the experimental results and the prediction values of the bead height and bead width using equation (8). It can be seen that there are small deviations between the prediction values from the experimental results. With the parameter ranges and equation (8), the maximum bead area can be obtained, which is 8.62 mm² when $h = 2.704$ mm and $w = 4.872$ mm.

Due to the root opening, which makes it difficult for robotic welding, the root pass is assumed to be completed by manual welding, and it is excluded from the pass planning. Tables 2 and 3 summarize the pass planning results for the toe area and the heel area, respectively, including the number of layers, the number of

passes and the associated welding parameters for each layer.

In planning the toe area, the four coefficients in equation (7) were set to $\omega_h = 0.1$, $\omega_w = 0.5$, $\omega_p = 0.3$

Table 1. Welding parameters and corresponding bead dimensions.

| Speed v (mm/min)	Voltage V (V)	Current I (A)	Bead height h (mm)	Bead width w (mm)
250	20	180	1.90	3.77
250	20	260	2.32	4.27
250	20	360	2.77	4.78
250	25	180	1.48	4.38
250	25	260	1.81	4.97
250	25	360	2.16	5.56
250	30	180	1.21	4.96
250	30	260	1.48	5.62
250	30	360	1.76	6.29
330	20	180	1.76	3.33
330	20	260	2.15	3.78
330	20	360	2.57	4.22
330	25	180	1.37	3.87
330	25	260	1.68	4.39
330	25	360	2.00	4.91
330	30	180	1.12	4.38
330	30	260	1.37	4.97
330	30	360	1.64	5.56
410	20	180	1.66	3.02
410	20	260	2.03	3.43
410	20	360	2.42	3.84
410	25	180	1.29	3.52
410	25	260	1.58	3.99
410	25	360	1.89	4.46
410	30	180	1.06	3.98
410	30	260	1.29	4.52
410	30	360	1.54	5.05
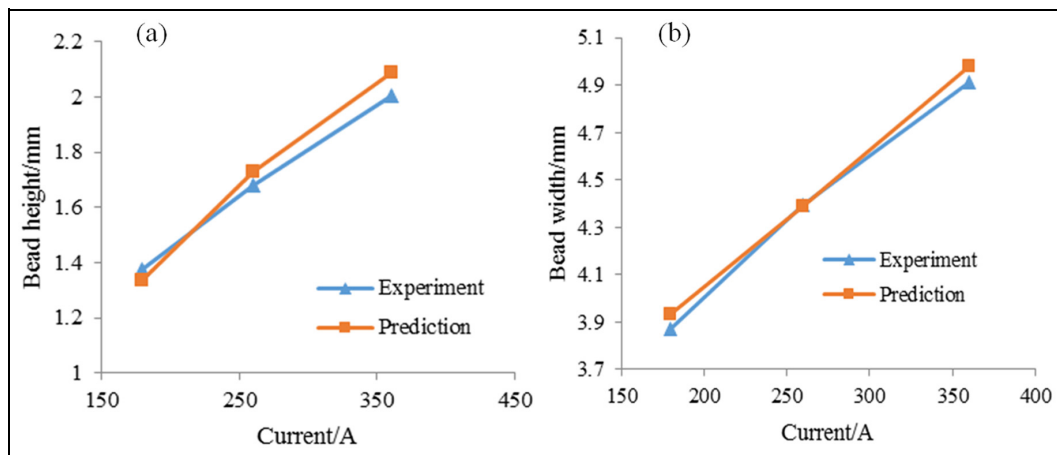
Figure 8. Experimental and prediction values for (a) bead height and (b) bead width, with 25 V voltage and 330 mm/min welding speed.

**Table 2.** Pass planning results for the toe area (of top-half groove).

Layer index	No. of passes	Bead height	Speed (mm/min)	Voltage (V)	Current (A)
1	2	1.936	330.9613	21.47429	245.7033
2	2	1.758	348.0911	21.59531	211.4183
3	3	1.469	319.6442	29.1552	277.4207
4	3	1.848	330.0317	21.69891	226.624
5	4	1.398	336.8391	25.63141	183.4607
6	4	1.835	350.6591	26.56263	336.2889
7	5	1.596	337.1999	23.99074	207.4222
8	6	1.483	314.7134	27.37562	235.3426
9	6	2.084	320.6152	24.91767	352.4723
10	7	1.589	317.313	29.66551	301.7797
11	7	1.334	337.0322	21.07912	209.8476

Table 3. Pass planning results for the heel area (of top-half groove).

Layer index	No. of passes	Sections included	Bead height (mm)	Speed (mm/min)	Voltage (V)	Current (A)
1	1	19–51	1.690	276.3528	22.882	187.369
2	2		1.738	342.7437	20	180
3	2		1.719	339.533	20.599	183.291
4	2		1.615	326.373	26.957	270.441
5	3		1.946	334.909	20	223.817
6	3		1.880	323.525	23.047	257.629
7	4		1.844	325.764	20	196.899
8	4		1.451	345.983	24.884	188.167
9	5		1.758	331.002	20	180
10	5		1.513	335.536	22.154	180.059
11	6		1.743	339.408	20	180
12	4	40–51	2.077	330.556	24.291	338.978
13	4	42–51	1.443	315.125	27.629	228.864
14	4	43–51	1.935	331.297	21.662	272.115
15	4	44–51	1.584	343.899	23.279	194.543
16	5	45–51	1.687	291.301	27.339	288.036
17	5		1.498	316.824	27.854	252.201
18	5	46–51	2.122	354.788	20.082	272.870
19	5	47–51	1.788	304.149	20.831	188.533
20	5		2.207	332.237	22.123	323.286
21	6	48–51	2.298	302.329	21.072	311.002
22	6		2.229	341.383	20	290.143
23	6	49–51	2.085	303.587	20	242.516
24	6		2.334	349.587	20	316.864
25	7		2.159	281.858	21.710	282.896
26	7	50–51	2.151	298.795	20	255.227
27	7		2.213	381.096	20	302.698
28	8		1.847	360.097	21.410	258.133
29	8		1.935	328.907	20.003	218.903
30	8	51	1.801	328.934	20	188.732
31	8		1.954	259.799	20	230.784

Table 4. Selection of weighted coefficients.

Group	1	2	3	4	5
w_w	0.5	0.6	0.7	0.75	0.79
w_p	0.3	0.2	0.1	0.05	0.01
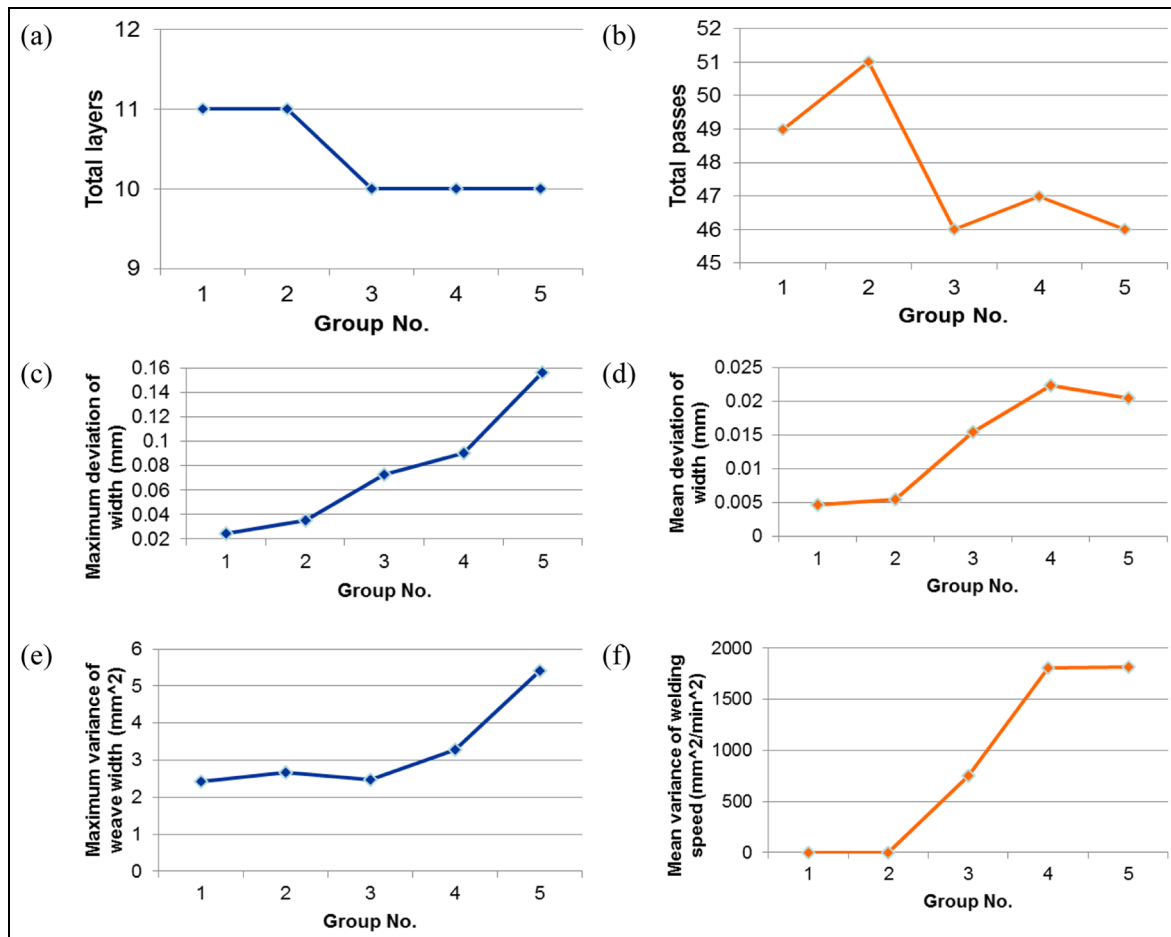
Figure 9. Pass results in comparison with the section of weighted coefficients in toe area: (a) total number of layers, (b) total number of passes, (c) maximum deviation of bead width, (d) mean deviation of bead width, (e) maximum variance of weave width and (f) mean variance of weave width.

and $\omega_a = 0.1$. The entire toe segment can be filled up with equal number of layers and passes, that is, 11 layers and 49 passes in total. In planning the heel area, the four coefficients in equation (7) were set to $\omega_h = 0.1$, $\omega_w = 0.7$, $\omega_p = 0.1$ and $\omega_a = 0.1$. The heel segment requires 31 layers and 155 passes in total. In particular, after 11 layers, half of the heel segment can be filled up, and the remaining portion can be gradually filled up with more layers. Both toe and heel segments allow weaving to reduce the total number of passes needed. Layers 12–15 have fewer passes than the previous layer (layer 11) due to the increase in their weave width.

Discussion

The effects of the selection of weighted coefficients in equation (7) on the smoothness of the resulting welding parameters and weld bead shape were investigated. As the objectives on minimizing the bead height (f_h) and maximizing the bead sections (f_a) are relatively less important, the two coefficients associated were set to 0.1. The other two coefficients w_w and w_p were investigated in detail. A total of five set of values of these two coefficients are given in Table 4, and the pass results in comparison with the section of weighted coefficients in the toe area and heel area are illustrated in Figures 9 and 10.

It can be concluded based on Figures 9 and 10 that among the five groups of coefficients, group 1 gives the best option for the coefficients for the toe area with which the total numbers of layers and passes are slightly larger than the minimum values, while the deviation of bead width, the variance of weave width and welding speed have the least values. Group 3 gives the best
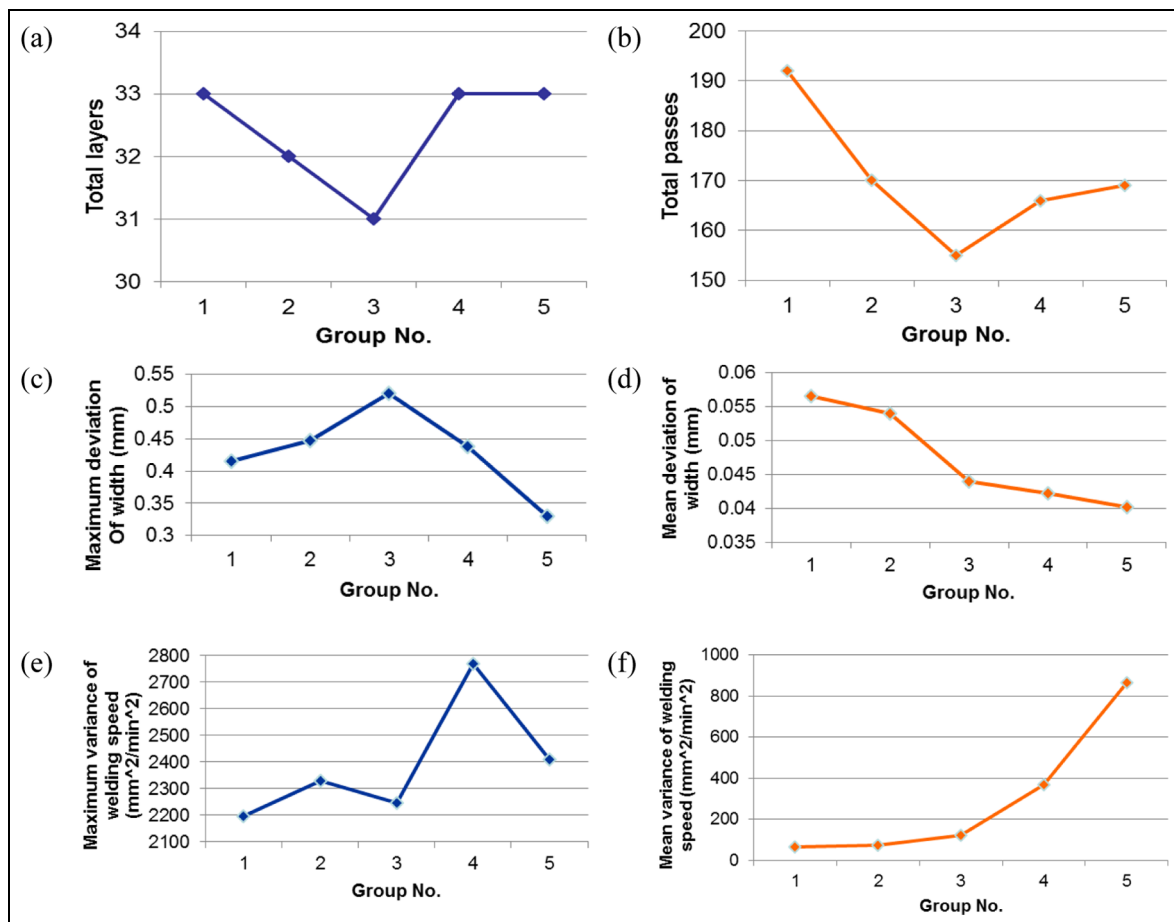
Figure 10. Pass result in comparison with the section of weighted coefficients in heel area: (a) total number of layers, (b) total number of passes, (c) maximum deviation of bead width, (d) mean deviation of bead width, (e) maximum variance of weave width and (f) mean variance of weave width.

selection of the coefficients for the heel area with which the total numbers of layers and passes are the smallest, and the mean deviation of bead width variance of weave width and welding speed is moderate compared to the other four options of weighted coefficients.

Conclusion

The welding parameter knowledge database is able to provide accurate welding bead geometry prediction models. The models can be used to predict bead shapes with the given welding parameters. The welding parameters can also be obtained to achieve defined bead shapes using the prediction models.

The optimization algorithm for pass planning maximizes the section areas of the weld bead in every layer to achieve minimal number of welding passes. Optimization constraints are applied to maintain consistent welding parameters for each welding layer as well as for each individual welding pass. The planning result provides the number of layers, number of passes in each layer and the corresponding welding parameters. The case study shows that the proposed method is able to provide feasible solutions for the pass planning of a nonuniform groove, and the weld beads

of all the passes can be achieved using feasible welding parameters.

References

1. Chen C, Hu S, He D, et al. An approach to the path planning of tube–sphere intersection welds with the robot dedicated to J-groove joints. *Robot Cim: Int Manuf* 2013; 29(4): 41–48.
2. Yang C, Ye Z, Chen Y, et al. Multi-pass path planning for thick plate by DSAW based on vision sensor. *Sensor Rev* 2014; 34(4): 416–423.

3. Micallef K, Fang G and Dinham M. Automatic seam detection and path planning in robotic welding. In: T-J Tarn, S-B Chen and G Fang (eds) *Robotic welding, intelligence and automation* (Lecture notes in electrical engineering), vol. 88. Berlin; Heidelberg: Springer, 2011, pp.23–32.

4. Reinhart G, Munzert U and Vogl W. A programming system for robot-based remote-laser-welding with conventional optics. *CIRP Ann: Manuf Techn* 2008; 57(1): 37–40.

5. Vosniakos GC and Chronopoulos A. Industrial robot path planning in a constraint-based computer-aided design and kinematic analysis environment. *Proc IMechE, Part B: J Engineering Manufacture* 2009; 223(5): 523–533.

6. Fang HC, Ong SK and Nee AYC. Interactive robot trajectory planning and simulation using augmented reality. *Robot Cim: Int Manuf* 2012; 28(2): 227–237.

7. Pai YS, Yap HJ and Singh R. Augmented reality–based programming, planning and simulation of a robotic work cell. *Proc IMechE, Part B: J Engineering Manufacture* 2015; 229(6): 1029–1045.

8. Park JU and An GB. Effect of welding sequence to minimize fillet welding distortion in a ship's small component fabrication using joint rigidity method. *Proc IMechE, Part B: J Engineering Manufacture* 2016; 230(4): 643–653.

9. Liu Y and Zhang Y. Iterative local ANFIS-based human welder intelligence modeling and control in pipe GTAW process: a data-driven approach. *IEEE/ASME T Mech* 2015; 20(3): 1079–1088.

10. Manorathna P, Marimuthu S, Justham L, et al. Human behaviour capturing in manual tungsten inert gas welding for intelligent automation. *Proc IMechE, Part B: J Engineering Manufacture* 2017; 231: 1619–1627.

11. Cao Y, Zhu S, Liang X, et al. Overlapping model of beads and curve fitting of bead section for rapid manufacturing by robotic MAG welding process. *Robot Cim: Int Manuf* 2011; 27(3): 641–645.

12. Xiong J, Zhang G, Gao H, et al. Modeling of bead section profile and overlapping beads with experimental validation for robotic GMAW-based rapid manufacturing. *Robot Cim: Int Manuf* 2013; 29(2): 417–423.

13. Suryakumar S, Karunakaran KP, Bernard A, et al. Weld bead modeling and process optimization in Hybrid Layered Manufacturing. *Comput Aided Design* 2011; 43(4): 331–344.

14. Palani PK and Murugan N. Optimization of weld bead geometry for stainless steel claddings deposited by FCAW. *J Mater Process Tech* 2007; 190(1–3): 291–299.

15. Ganjigatti JP, Pratihar DK and Choudhury AR. Global versus cluster-wise regression analyses for prediction of bead geometry in MIG welding process. *J Mater Process Tech* 2007; 189(1–3): 352–366.

16. Kolahan F and Heidari M. Modeling and optimization of MAG welding for gas pipelines using regression analysis and simulated annealing algorithm. *J Sci Ind Res India* 2010; 69: 259–265.

17. Xiong J, Zhang J, Hu J, et al. Bead geometry prediction for robotic GMAW-based rapid manufacturing through a neural network and a second-order regression analysis. *J Intell Manuf* 2014; 25(1): 157–163.

18. Ganjigatti JP, Pratihar DK and Choudhury AR. Modeling of the MIG welding process using statistical approaches. *Int J Adv Manuf Tech* 2008; 35(11–12): 1166–1190.

19. Kim IS, Son JS, Kim IG, et al. A study on relationship between process variables and bead penetration for robotic CO_2 arc welding. *J Mater Process Tech* 2003; 136(1–3): 139–145.

20. Kim IS, Son JS and Yarlagadda PKDV. A study on the quality improvement of robotic GMA welding process. *Robot Cim: Int Manuf* 2003; 19(6): 567–572.

21. Thao DT, Kim IS, Na HH, et al. Development of mathematical model with a genetic algorithm for automatic GMA welding process. *Int J Adv Manuf Tech* 2014; 73(5–8): 837–847.

22. Lee JI and Um KW. A prediction of welding process parameters by prediction of back-bead geometry. *J Mater Process Tech* 2000; 108: 106–113.

23. Katherasan D, Elias JV, Sathiya P, et al. Simulation and parameter optimization of flux cored arc welding using artificial neural network and particle swarm optimization algorithm. *J Intell Manuf* 2012; 25(1): 67–76.

24. Singh A, Cooper DE, Blundell NJ, et al. Modelling of weld-bead geometry and hardness profile in laser welding of plain carbon steel using neural networks and genetic algorithms. *Int J Comput Integ M* 2013; 27(7): 656–674.

25. Campbell SW, Galloway AM and McPherson NA. Artificial neural network prediction of weld geometry performed using GMAW with alternating shielding gases. *Weld J* 2012; 91(6): 174–181.

26. Kim I, Son J, Park C, et al. A study on prediction of bead height in robotic arc welding using a neural network. *J Mater Process Tech* 2002; 130–131: 229–234.

27. Nagesh DS and Datta GL. Prediction of weld bead geometry and penetration in shielded metal-arc welding using artificial neural networks. *J Mater Process Tech* 2002; 123(2): 303–312.

28. Yan SJ, Ong SK and Nee AYC. Optimal pass planning for robotic welding of large-dimension joints with deep grooves. *Proc CIRP* 2016; 56: 188–192.

29. Rampaul H. *Pipe welding procedures.* 2nd ed. New York: Industrial Press, 2002.

Appendix I

Notation

B	ranges of welding parameters
f_a	reciprocal of the mean of the areas of bead sections
f_h	square root of the square sum of the differences of bead height
f_p	sum of standard deviations of welding speed and weave width
f_w	square root of the square sum of the differences of bead width
h	bead height
h_i	bead height of ith layer
h_g	distance from the bottom surface of current layer to the top surface of the groove
$H(\mathbf{X})$	prediction model of bead height
I	current
n	number of passes
N	number of cross sections

$P_1, P_2,$	intersection points of the layer surfaces	w_i	bead width of the ith pass
P_3, P_4	and the groove edges	$W(\mathbf{X})$	prediction model of bead width
S	area of an enclosed shape		
V	voltage	ε	tolerance
x_i	location of the ith pass in the x direction	ν	welding speed
$\mathbf{X}$	welding parameter vector	$\omega_h, \omega_w,$	weighted coefficients associated with $f_h,$
X_{Pi}	x coordinate of the intersection point P_i	ω_p, ω_a	f_w, f_p and $f_a,$ respectively
w	bead width		